Supporting Information for

Structure of the mammalian TRPM7, a magnesium channel required during embryonic development

Jingjing Duan[1]* , Zongli Li[2]*, Jian Li[3,4], Raymond E. Hulse[1,5], Ana Santa-Cruz[1,5], William C. Valinsky[5], Sunday A. Abiria[1], Grigory Krapivinsky[1], Jin Zhang[3#] and David E. Clapham[1,5,6#]

Affiliations:

[1]Howard Hughes Medical Institute, Department of Cardiology, Boston Children's Hospital, Enders Building 1309, 320 Longwood Avenue, Boston, MA 02115, USA.

[2]Howard Hughes Medical Institute, Department of Biological Chemistry and Molecular Pharmacology, Harvard Medical School, Boston, MA 02115, USA.

[3]School of Basic Medical Sciences, Nanchang University, Nanchang, Jiangxi, 330031, China.

[4]Department of Molecular and Cellular Biochemistry, University of Kentucky, Lexington, Kentucky 40536, USA.

[5]Howard Hughes Medical Institute, Janelia Research Campus, Ashburn, VA 20147, USA.

[6]Department of Neurobiology, Harvard Medical School, 220 Longwood Avenue, Boston, MA 02115, USA.

*These authors contributed equally to this work.

[#] Corresponding authors zhangxiaokong@hotmail.com (J.Z.), claphamd@hhmi.org (D.E.C.)

www.pnas.org/cgi/doi/10.1073/pnas.1810719115

Figure legends of supplementary figures

Fig. S1. Biochemical and electrophysiological properties of the truncated TRPM7 construct used for structural investigation.

(**a**) Size exclusion chromatography trace of the MBP-tagged truncated mouse TRPM7 protein. Void volume and peak corresponding to tetrameric channels are indicated. Protein samples of the indicated TRPM7 protein fraction were subjected to SDS–PAGE and Coomassie-blue staining. (**b)** Representative micrograph of the negatively-stained image of the TRPM7 protein. (**c**) Whole-cell I-V relationship of HEK293T TRPM6/7 double KO cells transiently transfected with EGFP (gray) or the MBP-tagged truncated mouse TRPM7 construct (mTRPM7; black). Inward current and reversal potential are shown in the inset. (**d**) Mean current density at +100 mV (top) and -100 mV (bottom) of the conditions described in A (n = 3 EGFP; n = 7 mTRPM7). (**e**) Representative recording of current growth over time at +100 mV (black) and -100 mV (gray) during whole-cell dialysis. (**f**) Plot of time-to-peak current at +100 mV (n = 7). (**g**) Whole-cell recording of mTRPM7 transfected cells elicited from the step protocol (21 steps of 500 ms duration in increments of +10 mV from -100 mV to +100 mV). (**h**) Whole-cell I-V relationship of mTRPM7 transfected cells before (2 mM Ca^{2+}; black), and after (110 mM Mg^{2+}; violet) perfusion of the high Mg^{2+} solution. Inward current and reversal potential are shown in the inset. (**i**) Current density at +90 mV for the conditions described in F (n = 5). Current is presented in nA and current density in pA/pF. Averaged data are presented as mean ± SEM.

Fig. S2. Flow chart for cryo-EM data processing.

Cryo-EM data processing of TRPM7-EDTA (**a**), TRPM7-Mg^{2+} (**b**), and TRPM7-DVF (**c**). These show representative images of the purified TRPM7 protein, 2D class averages of TRPM7 particles, side views of the 3D reconstructions from RELION 3D classification, final reconstructions from 3D auto-refinement, Fourier shell correlation (FSC) curves for the 3D reconstructions, local resolution maps (from ResMap (1)) and Euler distribution plots of particles used in the final three-dimensional reconstructions, with regions in red denoting the views containing the highest number of particles.

Fig. S3. Cryo-EM densities of selected regions of TRPM7.

Density maps showing the transmembrane helices (S1-6), TRP domain and coiled-coil domain of TRPM7-Mg^{2+} (top), TRPM7-DVF (middle), and TRPM7-EDTA (bottom). The maps were contoured at a level of 5.0 σ.

Fig. S4. Comparison of the transmembrane domains of TRPM7 with other known TRP channel structures.

Side views of the channel transmembrane domain monomers for TRPM7-Mg^{2+} (pink, PDB: 6BWD), TRPV1 (cyan, PDB:3J5P), TRPA1 (green, PDB:3J9P), PKD2 (polycystin-2; blue, PDB:5T4D), and TRPML1 (orange, PDB:5WPV; left). TRPM7-Mg^{2+} and TRPV1 are directly compared at right.

Fig. S5. Comparison of TRPM7 with other known TRPM structures.

(**a**) Superimposed side views of TRPM7-Mg^{2+} (blue, PDB:6BWD), TRPM4 (gray, PDB:6BWI), TRPM2 (yellow, PDB:6CO7) and TRPM8 (green, PDB:6BPQ) monomers, showing overall

similarity in these structures. Regions of the (**b**) S2-S3 helix and (**c**) pre-S1 helix are enlarged. Intracellular domains of TRPM structures including the (**d**) N and (**e**) C termini are aligned for comparison. N termini are shown with the linker-helical domain (LH), ankyrin-repeat domain (AR) and the N-terminal domain (NT). C termini are shown with the connecting helices (CH) and coiled-coil domain (CC).

Fig. S6. Sequence alignment of TRPM7 to TRPM family members.

Regions of the C terminus (a.a. 1150-1280) of mouse (**a**) and human (**b**) TRPM7 to other TRPM family members are shown with the connecting helix (a.a. 1165-1189) and the coiled-coil domain (a.a. 1194-1224) highlighted in boxes. The pore domain of TRPM7 mouse (**c**) and human (**d**) were aligned with other TRPM members. Regions corresponding to the pore helix (a.a. 1031-1043) are boxed. The selectivity filter (yellow), lower gate (yellow), and two highly conserved cysteines are (red circles) marked. Sequence alignments used Clustal Omega.

Fig. S7. Comparison of the ion conducting pathway in TRPM7 structures with other available TRPM structures.

(**a**) The conduction pathway of TRPM7-Mg^{2+} (blue), TRPM7-DVF (pink) and TRPM7-EDTA (orange) are compared; distances between specific side chains along the pore are listed. (**b**) The pore regions of TRPM7 (TRPM7-Mg^{2+}, blue), TRPM4 (gray) and TRPM2 (yellow) are compared with key residues labeled. (**c**) Superimposed side views of (b).

Fig. S8. Density maps of the TRPM7-Mg^{2+} and TRPM7-EDTA structures at the Mg^{2+}-binding site.

Density map of TRPM7-Mg^{2+} (blue) shown at three different contour levels: σ=3 (**a**), σ=4 (**c**) and σ=5 (**e**). Density map of TRPM7-EDTA (pink) shown at three different contour levels: σ=3 (**b**), σ=4 (**d**) and σ= 5 (**f**).

Table S1. Cryo-EM data collection, refinement and validation statistics

	TRPM7-Mg^{2+} (EMD-7297) (PDB 6BWD)	TRPM7-DVF (EMD-7298) (PDB 6BWF)	TRPM7-EDTA (EMD-6975) (PDB 5ZX5)
Data collection and processing			
Magnification	40607	40607	40607
Voltage (kV)	300	300	300
Electron exposure (e–/Å^2)	52.8	52.8	52.8
Defocus range (μm)	1.5-3.0	1.5-3.0	1.5-3.0
Pixel size (Å)	1.23	1.23	1.23
Symmetry imposed	*C4*	*C4*	*C4*
Initial particle images (#)	897,613	721,767	2,068,004
Final particle images (#)	232,930	206,032	1,039,775
Map resolution (Å)	3.7	4.1	3.28
FSC threshold			
Refinement			
Initial model used (PDB code)	*de novo*	*de novo*	*de novo*
Model resolution (Å)	3.7	4.1	3.28
FSC threshold			
Model composition			
Non-hydrogen atoms	25621	23944	25444
Protein residues	3236	3108	3256
Ligands	1	0	0
r.m.s. deviations			
Bond lengths (Å)	0.01	0.01	0.01
Bond angles (°)	1.27	1.51	1.60
Validation			
MolProbity score	2.03	2.02	1.73
Ramachandran plot			
Favored (%)	97.82	95.36	96.05
Allowed (%)	2.05	4.51	3.69
Disallowed (%)	0.13	0.13	0.26

References:

1. Kucukelbir, A., Sigworth, F.J. & Tagare, H.D. Quantifying the local resolution of cryo-EM density maps. *Nat Methods* **11**, 63-5 (2014).

Supplementary Fig. 1

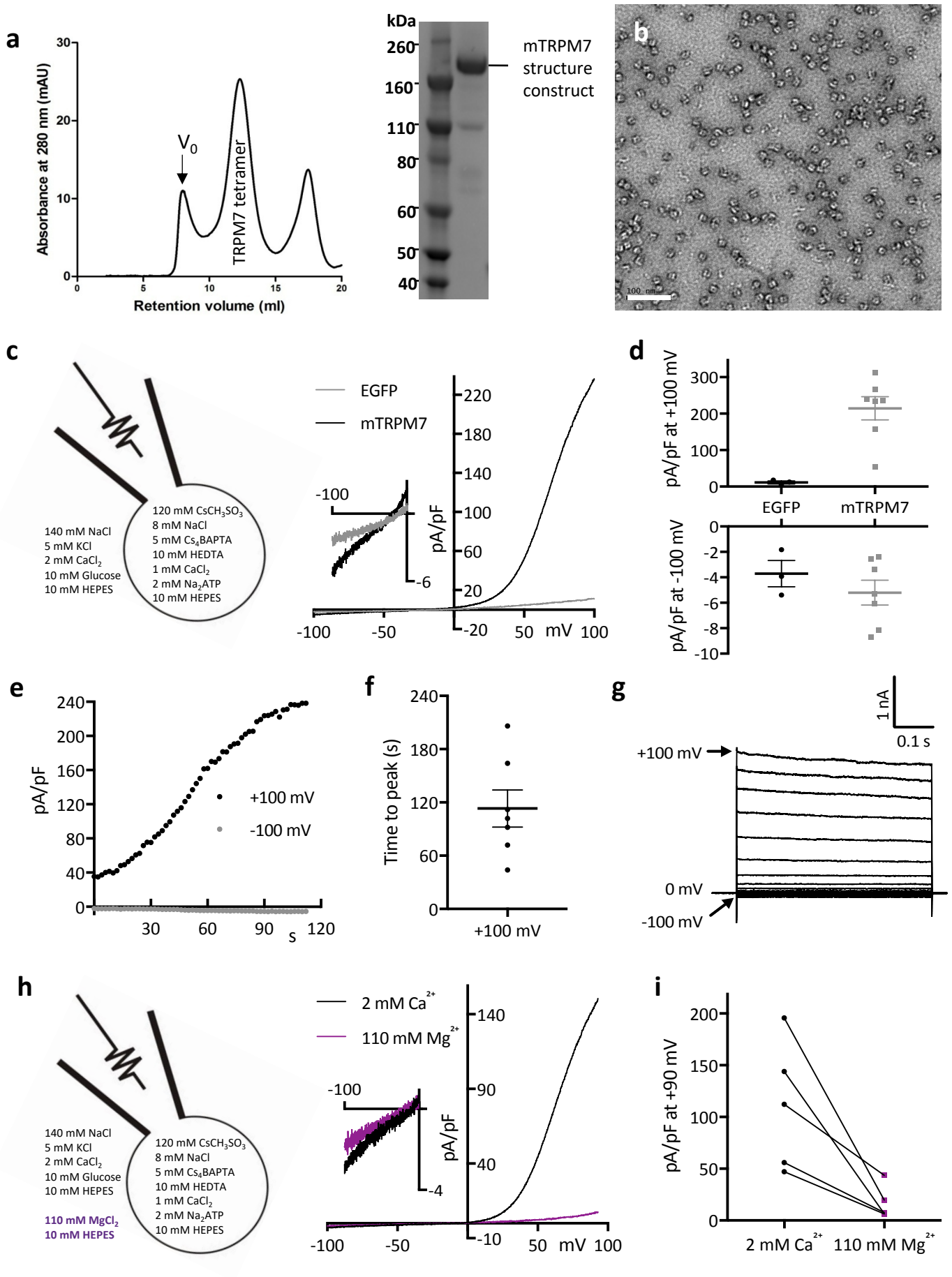

Supplementary Fig. 2

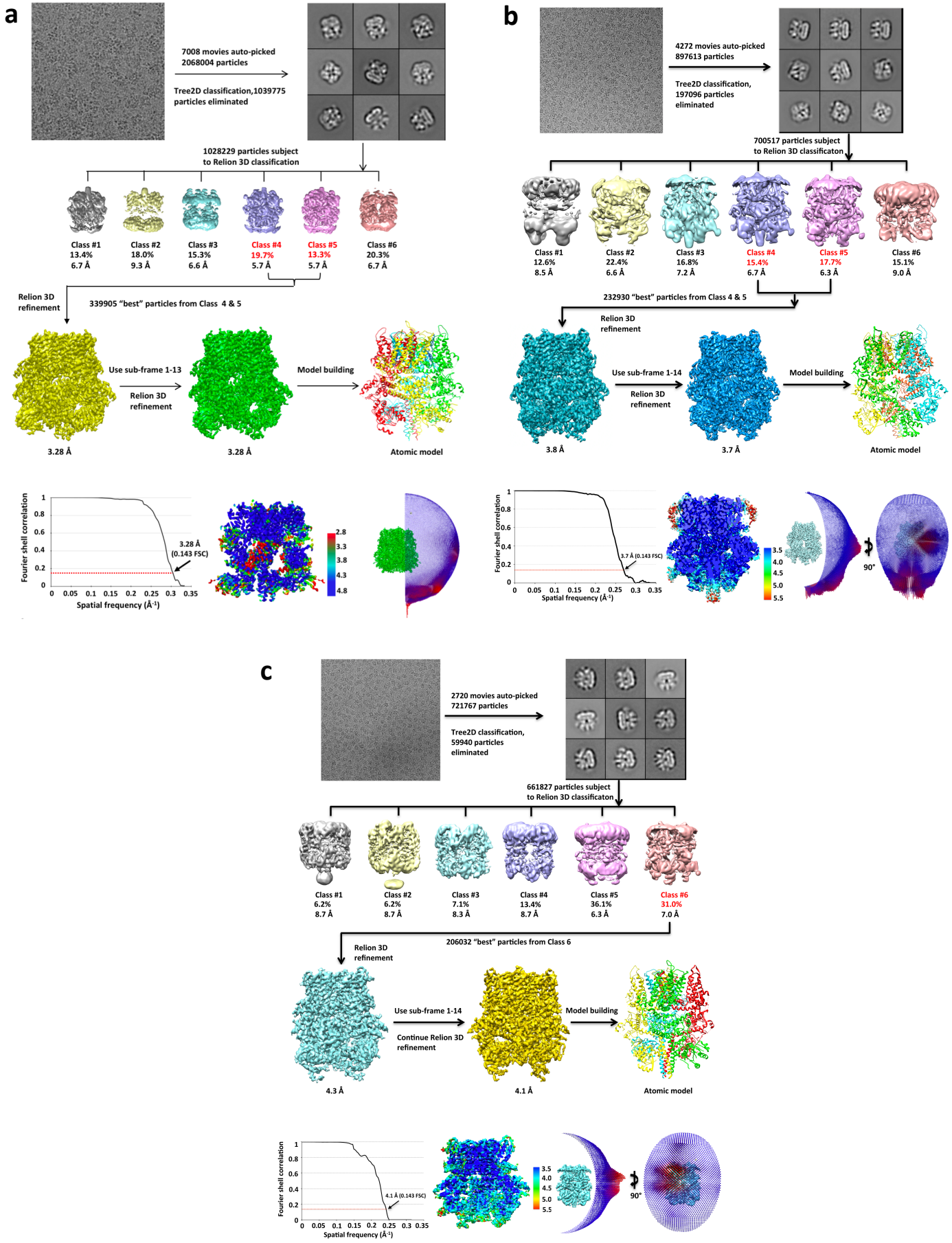

Supplementary Fig. 3

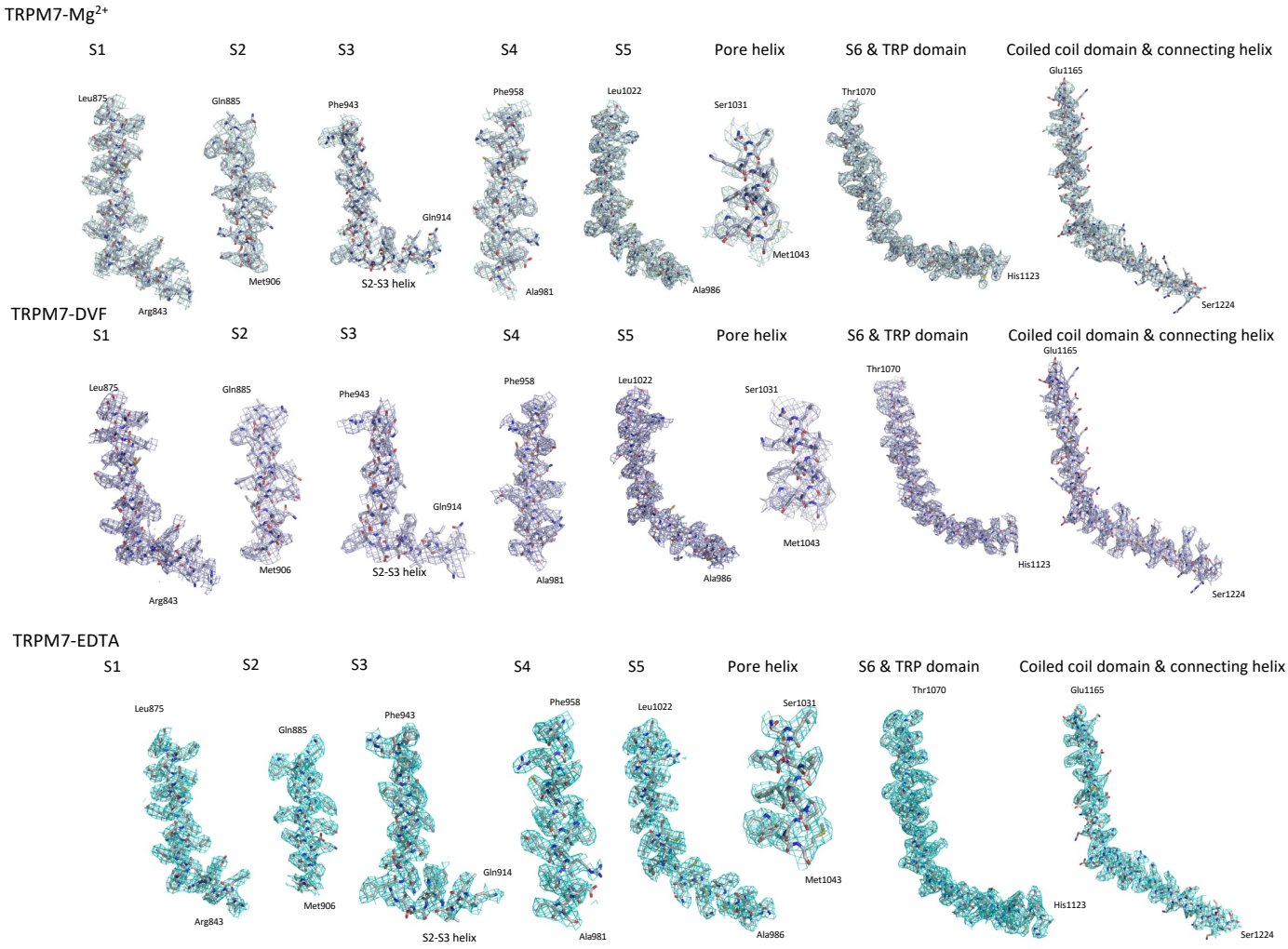

Supplementary Fig. 4

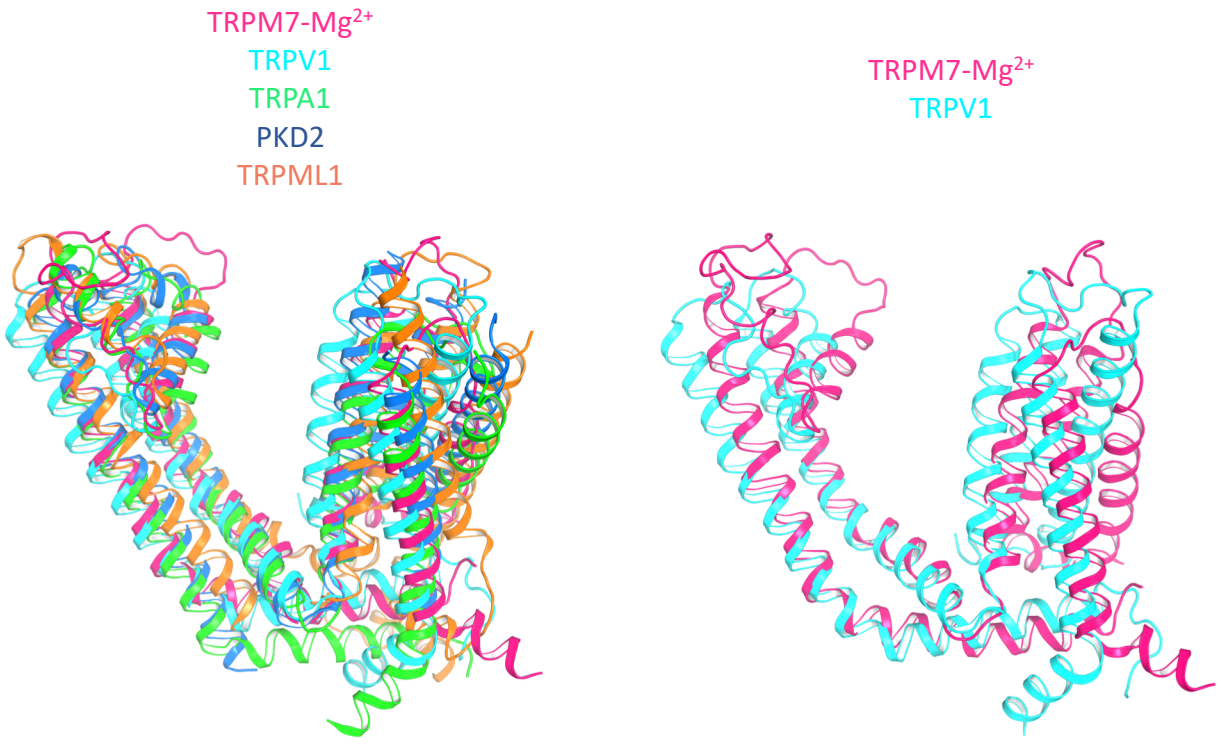

Supplementary Fig. 5

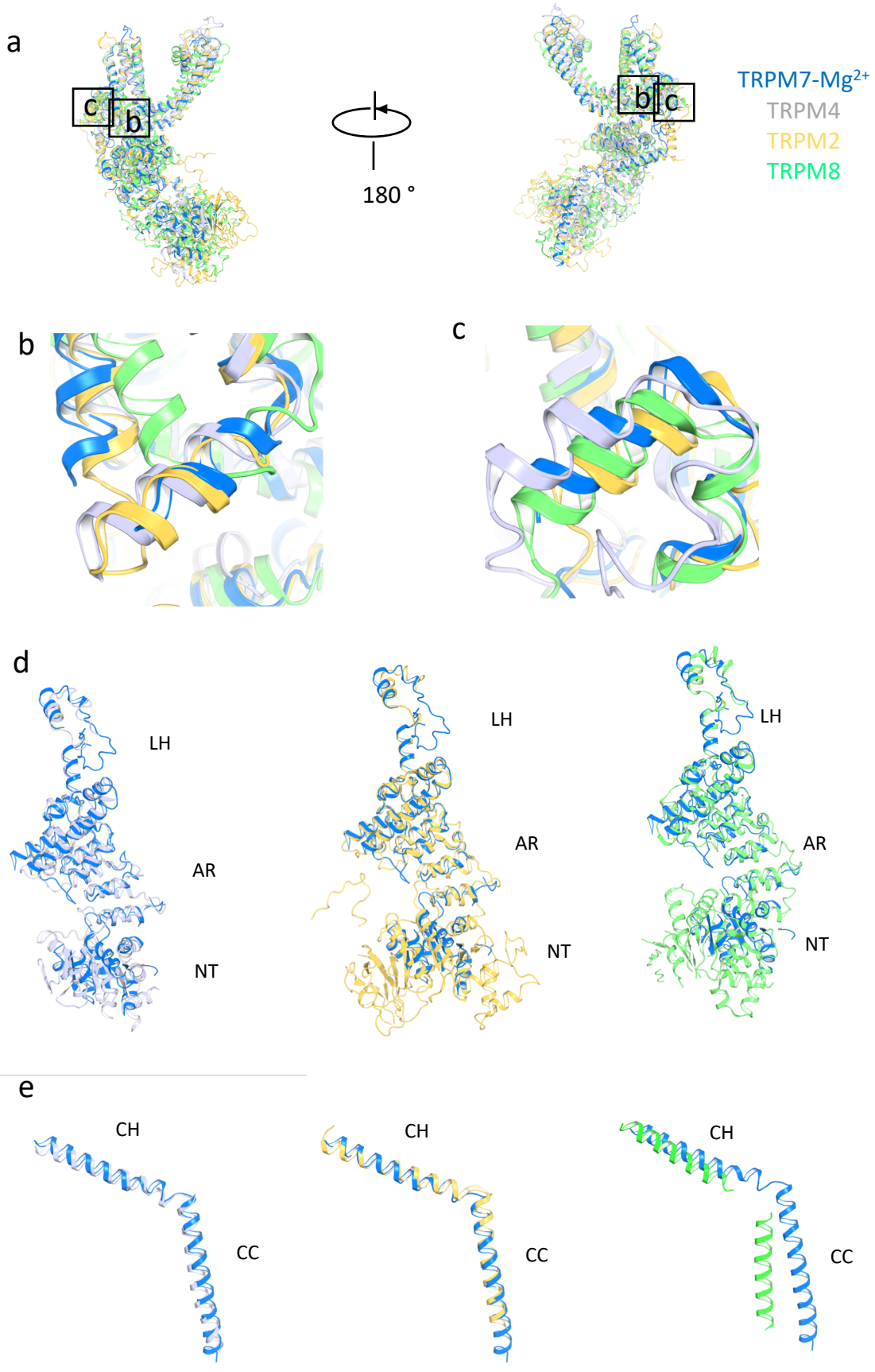

Supplementary Fig. 6a

a. Connecting helix and coiled-coil domain (TRPM7 mouse aa 1150-1280)

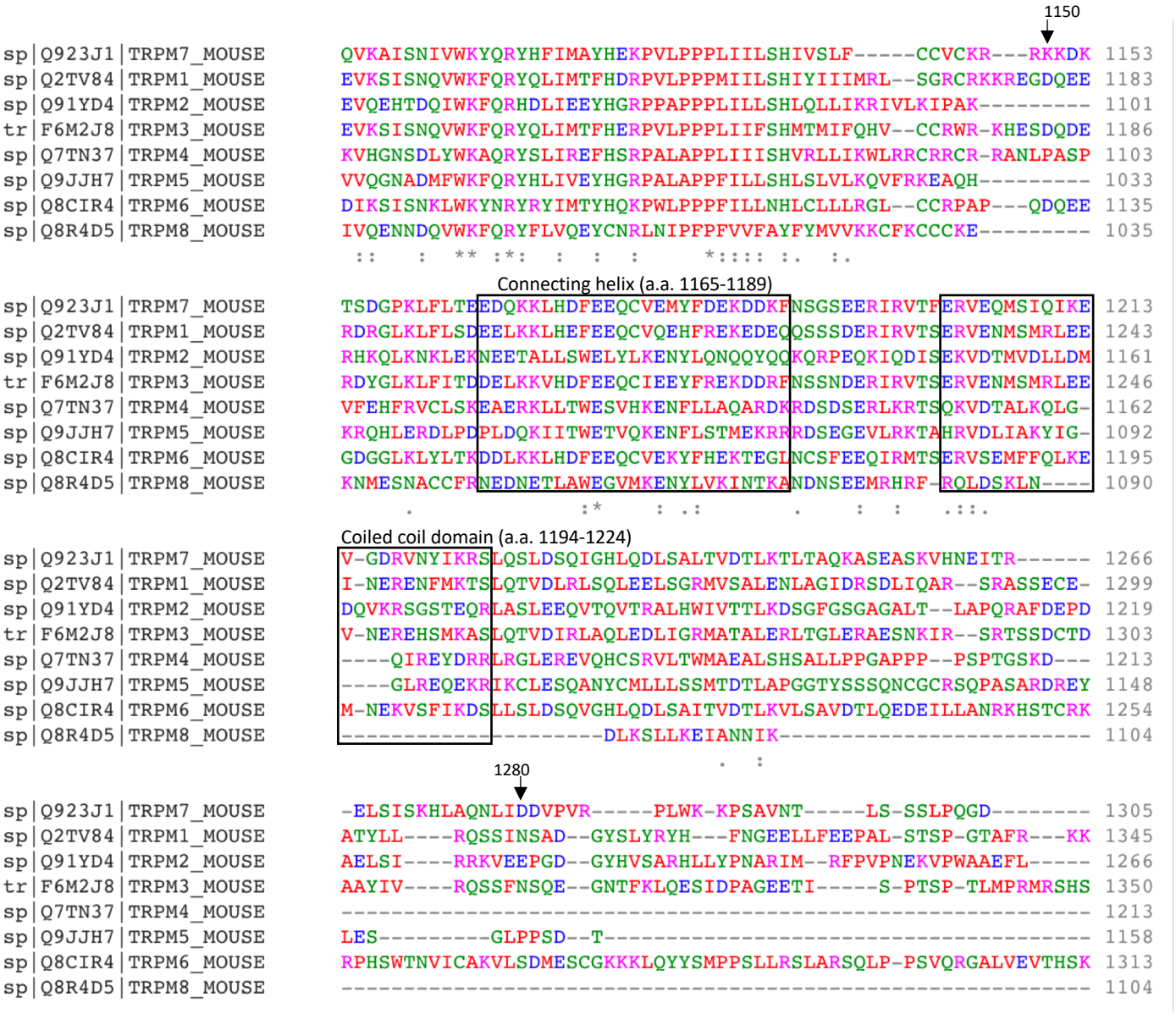

Supplementary Fig. 6b

b. Connecting helix and coiled-coil domain (TRPM7 human aa 1150-1280)

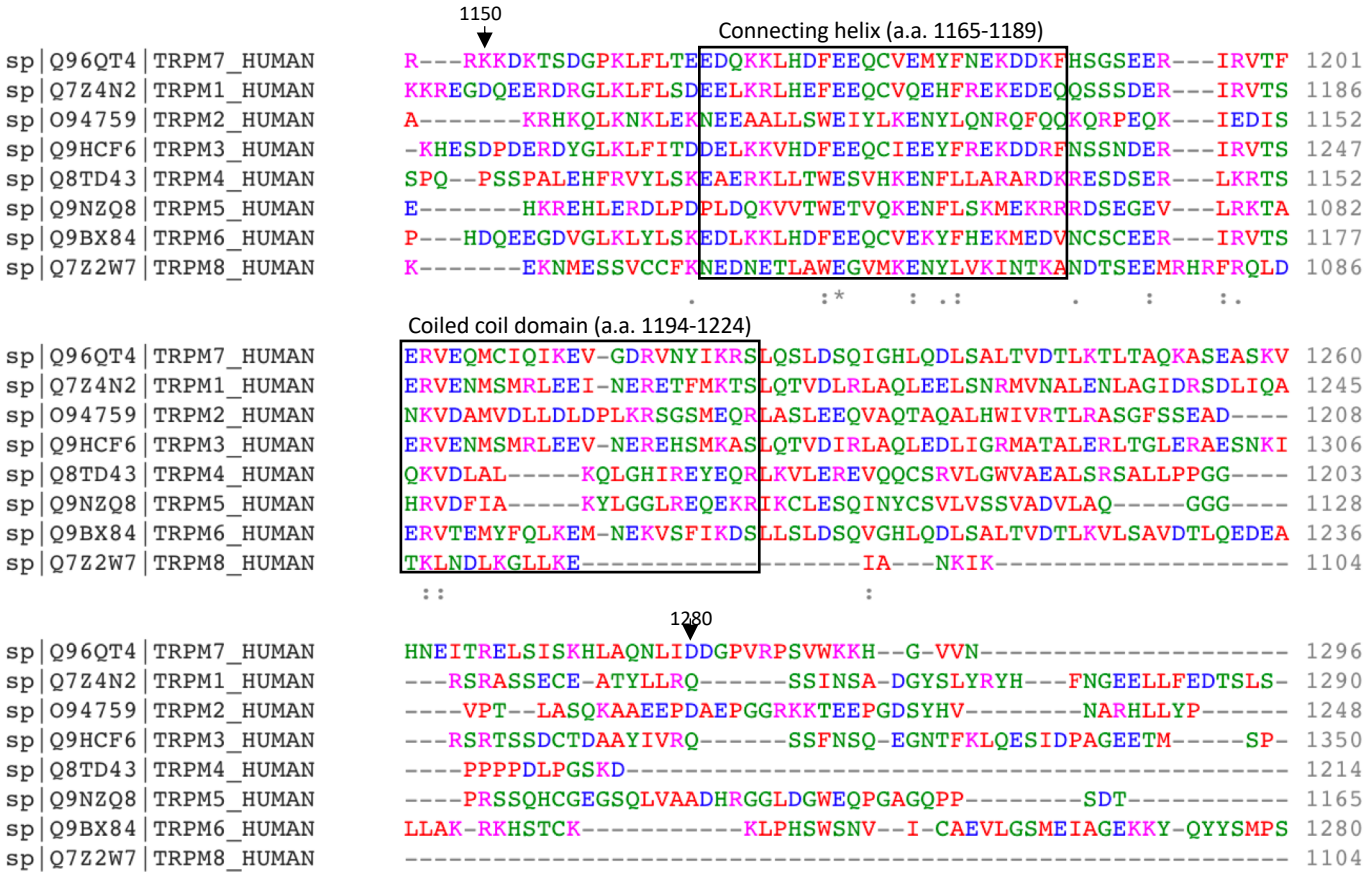

Supplementary Fig. 6c

c. Pore domain (TRPM7 mouse aa 1016-1100）

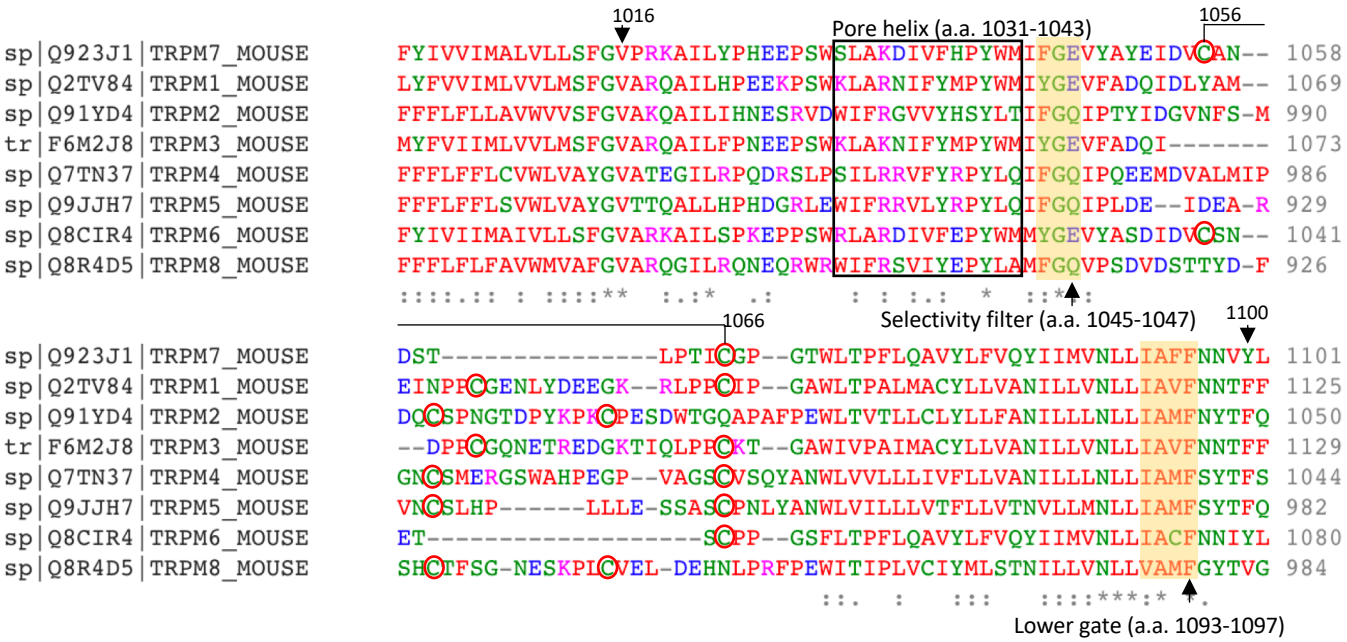

Supplementary Fig. 6d

d. Pore domain (TRPM7 human aa 1016-1100)

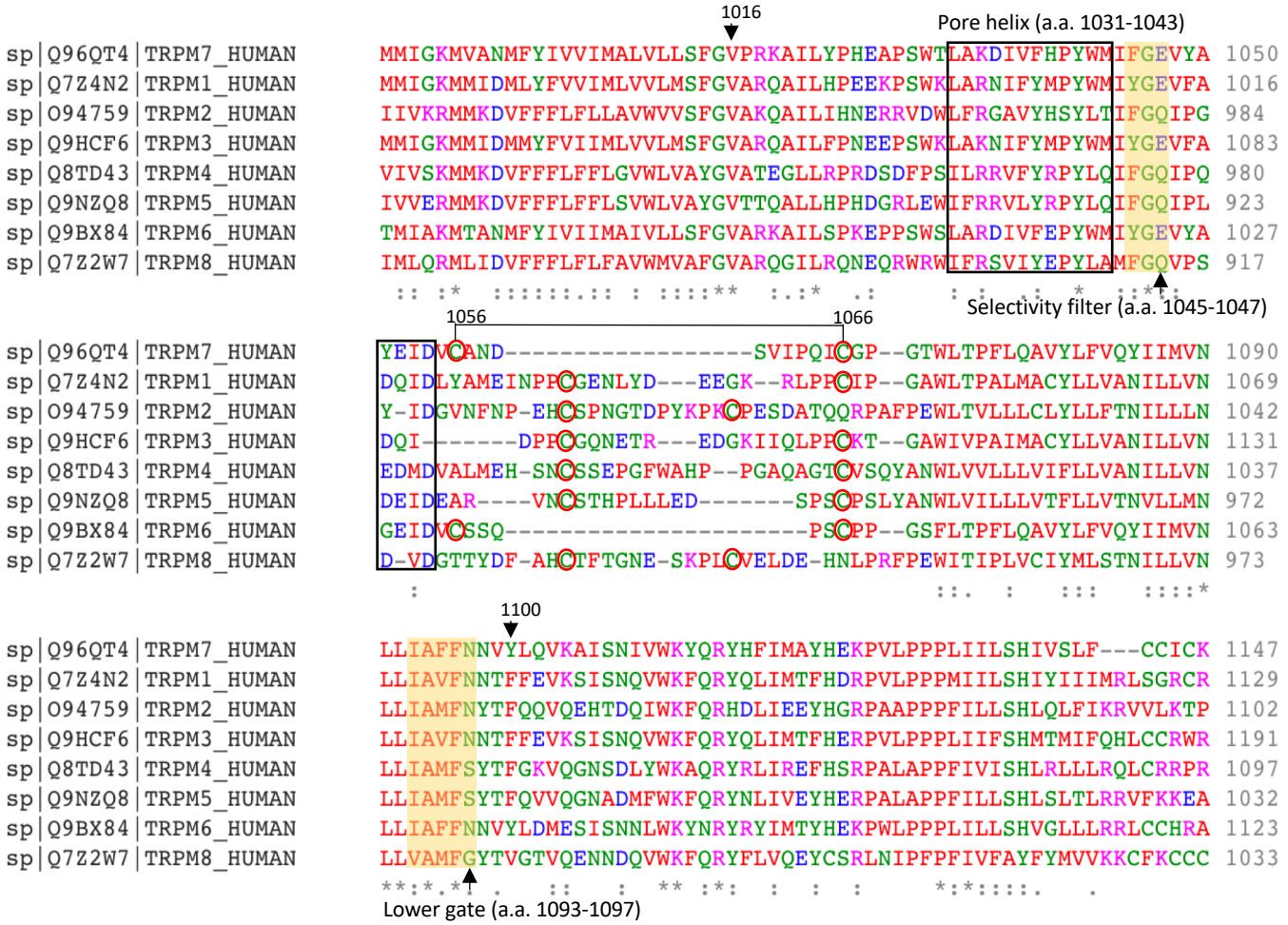

Supplementary Fig. 7

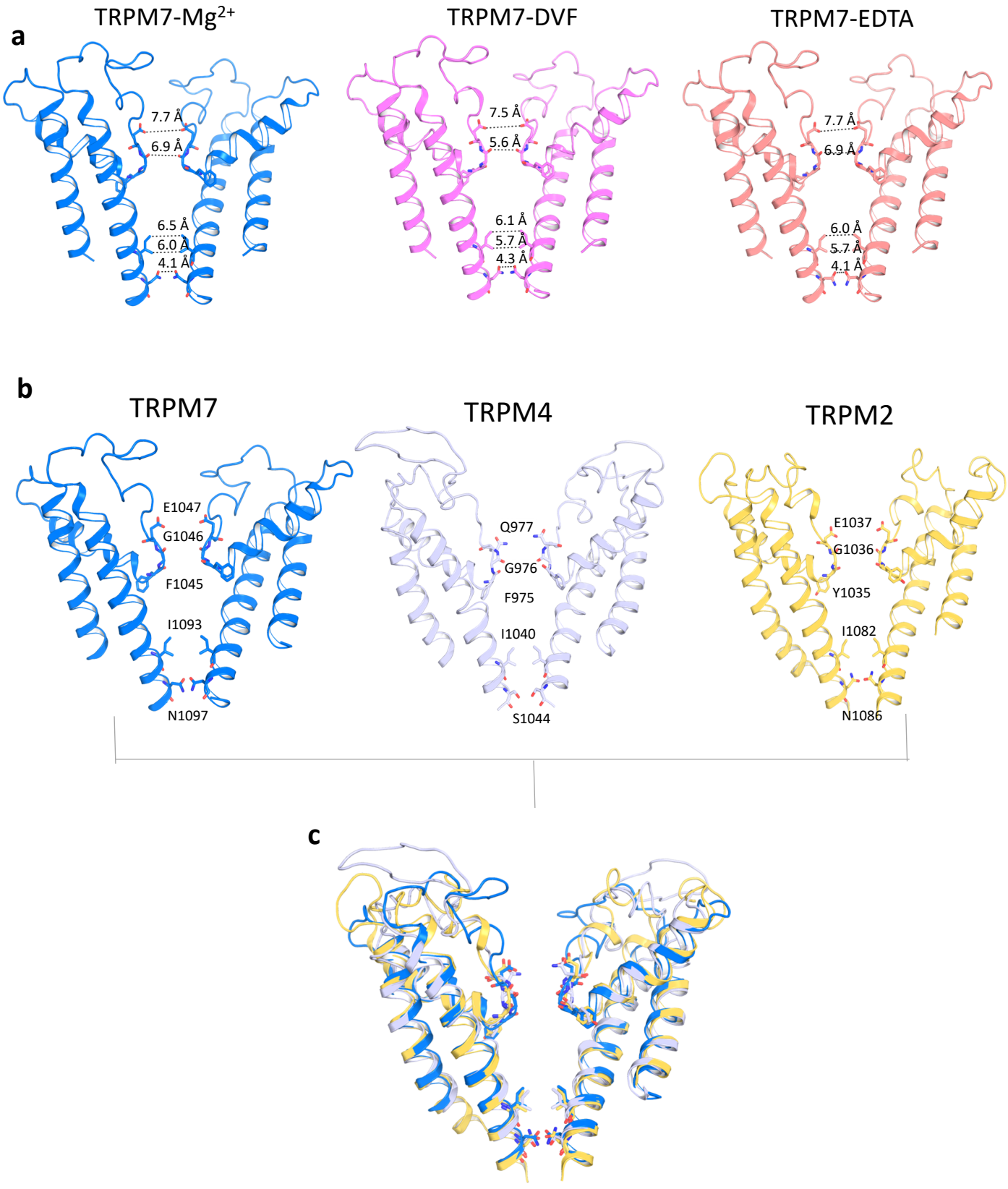
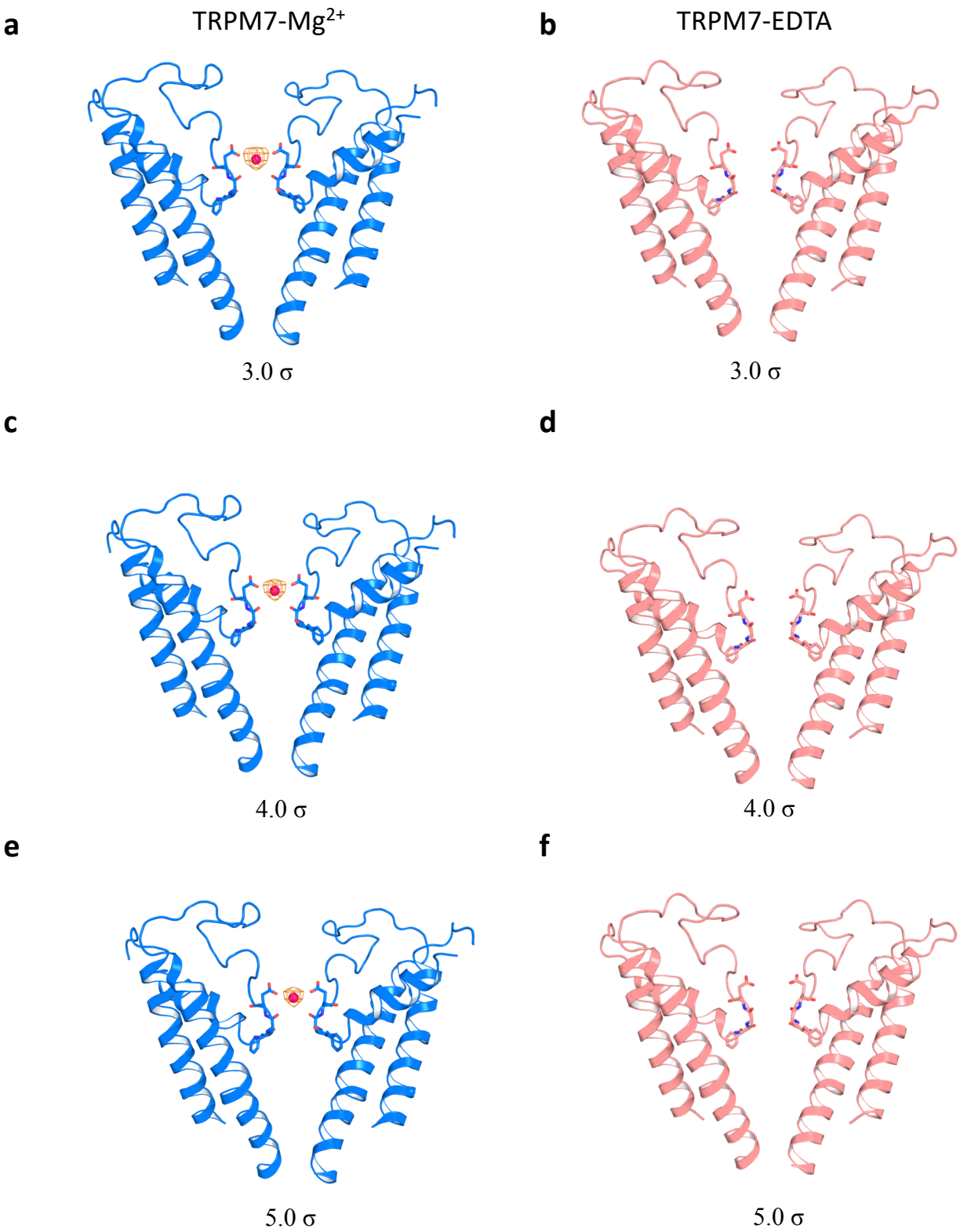
Supplementary Fig. 8